

Kinetics of the Reduction of Hematite Concentrate Particles by Carbon Monoxide Relevant to a Novel Flash Ironmaking Process



FENG CHEN, YOUSEF MOHASSAB, SHENGQIN ZHANG, and HONG YONG SOHN

A novel ironmaking process is under development at the University of Utah to produce iron directly from iron oxides concentrates by the gas–solid flash reaction using gaseous fuels and reductants. This process will reduce energy consumption and minimize carbon dioxide emissions. Having investigated the hydrogen reduction kinetics of magnetite and hematite concentrate particles relevant to the novel flash ironmaking process, the carbon monoxide reduction kinetics of hematite concentrate particles (average particle size 21 μm) was determined in the temperature range 1473 K to 1623 K (1200 °C to 1350 °C) under various carbon monoxide partial pressures. At 1623 K (1350 °C) and residence time 5 seconds, the reduction degree of hematite concentrate particles was more than 90 pct under a pure carbon monoxide. This is slower than reduction by hydrogen but still significant, indicating that CO will contribute to the reduction of hematite concentrate in the flash process. The kinetics of CO reduction separately from hydrogen is important for understanding and analyzing the complex kinetics of hematite reduction by the $\text{H}_2 + \text{CO}$ mixtures. The nucleation and growth rate equation with the Avrami parameter $n = 1.0$ adequately described the carbon monoxide reduction kinetics of hematite concentrate particles. The reduction rate is of 1st order with respect to the partial pressure of carbon monoxide and the activation energy of the reaction was 231 kJ/mol, indicating strong temperature dependence. The following complete rate equation was developed that can satisfactorily predict the carbon monoxide reduction kinetics of hematite concentrate particles and is suitable for the design of a flash reactor $\frac{dX}{dt} = 1.91 \times 10^7 \times e^{\frac{-231000}{RT}} \times \left(p\text{CO} - \frac{p\text{CO}_2}{K} \right) \times (1 - X)$, where X is the fraction of oxygen removed from iron oxide, R is 8.314 J/mol K, T is in K, p is in atm, and t is in seconds.

DOI: 10.1007/s11663-015-0345-7

© The Minerals, Metals & Materials Society and ASM International 2015

I. INTRODUCTION

A large number of alternate ironmaking technologies have been developed or are under development with the aim to replace the blast furnace for its high energy consumption and CO_2 emissions. A large portion of these problems are due to the use of coke to start with and the needs of sintering, pelletization, and cokemaking steps associated with the blast furnace operation. A novel flash ironmaking process is under development at the University of Utah,^[1–7] in which iron ore concentrate is flash reduced by gaseous reductants at temperatures above about 1473 K (1200 °C). This flash

ironmaking process eliminates sintering, pelletization, and cokemaking steps of the blast furnace and other ironmaking processes, making it more energy efficient and drastically lowering the emissions of environmental pollutants, especially carbon dioxide.

Although hydrogen is the cleanest and most efficient reductant, other gaseous reductants can be used as well. Reformed natural gas and coal gas, which are mainly composed of CO and H_2 , are also possible reductants in this novel process.

Previous research on gaseous reduction of iron oxide by carbon monoxide has typically involved samples larger than concentrate particles, such as ore fines, sinter, and pellets. Further, the temperature range tested was substantially lower than in the new flash ironmaking process. Ray and Kundu^[8] determined that hematite reduction in CO-N_2 mixtures had an activation energy of 90 kJ/mol in the temperature range of 1073 K to 1273 K (800 °C to 1000 °C) using powder samples in a TG/DTA instrument. Dutta and Ghosh^[9] studied the reduction of “blue dust” (44 to 100 μm , 95.7 pct Fe_2O_3) by CO at 1073 K to 1373 K (800 °C to 1100 °C), and found that $\text{Ln } k_c$ (chemical rate constant) vs $1/T$ plots did not yield straight lines because of the structural changes during the reduction. Piotrowski *et al.*^[10] reduced hematite particles of 91 μm average size to wustite by carbon monoxide at 973 K to 1173 K (700 °C to

FENG CHEN, formerly a Visiting Ph.D Student with the Department of Metallurgical Engineering, University of Utah, Salt Lake City, UT 84112, is now a Ph.D Student in the School of Minerals Processing and Bioengineering, Central South University, Changsha, Hunan 410083, P.R.China. YOUSEF MOHASSAB, Research Associate, and HONG YONG SOHN, Professor, are with the Department of Metallurgical Engineering, University of Utah. Contact e-mail: h.y.sohn@utah.edu SHENGQIN ZHANG, a Visiting Professor with the Department of Metallurgical Engineering, University of Utah, is Assistant Professor with the School of Metallurgy and Materials Engineering, Chongqing University of Science and Technology, Chongqing 401331, P.R. China.

Manuscript submitted March 10, 2015.

Article published online April 18, 2015.

900 °C). The nucleation and growth kinetic model was applied to the initial stages of the reduction process, which gradually shifted to diffusion control as reduction proceeded. They determined activation energy to be 58 kJ/mol. Hematite pellets of mean diameter 1.07 and 1.24 cm were reduced by pure hydrogen, pure CO, and Midrex gas (H₂ 55.7 pct, CO 34 pct, CO₂ 6.3 pct and CH₄ 4.0 pct) at 1123 K (850 °C) by Bonalde and Henriquez.^[11] They found that chemical reaction and internal gas diffusion were competing processes in the first stage of reduction of hematite pellets with H₂ or CO, and then gas diffusion became controlling step at the last stage of the process. The reduction kinetics of hematite to magnetite in the temperature range of 723 K to 973 K (450 °C to 700 °C) and magnetite to wustite at temperatures of 923 K to 1173 K (650 °C to 900 °C) in carbon monoxide and carbon dioxide mixtures were investigated in a fluidized bed by Bohn and Cleeton.^[12] They found that both reactions, Fe₂O₃ to Fe₃O₄ and Fe₃O₄ to Fe_{0.947}O, were first order with respect to the concentration of CO and the activation energy was 75 ± 12 and 90 ± 29 kJ/mol, respectively. Mondal *et al.*^[13] investigated the reduction of hematite powder by a continuous stream of CO in the temperature range of 1073 K to 1173 K (800 °C to 900 °C) using thermogravimetric analysis, and obtained the values of activation energy of 9.97 kJ/mol when Fe₂O₃ reduced to Fe₃O₄ and 14.13 kJ/mol as Fe₃O₄ reduced to Fe_{0.947}O. The reduction of hematite fines (highly porous oxide, moderately porous oxides, and dense oxides) to wustite with a CO and CO₂ mixture at the temperatures of 863 K to 1273 K (590 °C to 1000 °C) was studied by Corbari and Fruehan.^[14] They found that in their experimental configuration external gas mass transfer controlled the first reduction step (Fe₂O₃ to Fe₃O₄), while the reduction mechanism of the second step (Fe₃O₄ to Fe_{0.947}O) varied with the temperature.

As can be seen from above, most of the previous work on the reduction of iron oxides was conducted at temperatures lower than the minimum temperature, 1473 K (1200 °C), expected for the new flash process. Furthermore, the majority focused on the reduction of hematite samples with particle size larger than <100 μm, which is significantly larger than the concentrate particles for the novel flash process. Additionally, in the rapid reduction of fine hematite particles at high temperatures, the reduction does not proceed by forming the next lower oxides in order; rather, a combination of hematite, magnetite, wustite, and iron is present at any given moment, as will be shown later. Thus, the reduction rate in this work was represented by the overall fraction of oxygen removed without distinguishing the reaction of different iron oxide phases. In the design of a reactor for the novel process such a global rate expression is sufficient.

There had been little work on the gaseous reduction of iron oxide concentrates before the conception of the new flash ironmaking technology.^[2,15,16] In conjunction with this development work, Sohn and coworkers^[2,15-17] have investigated the gaseous reduction of magnetite and hematite concentrate particles aimed at generating a database to be used for the design of a flash ironmaking reactor. Their work included the measurement of the intrinsic kinetics of the hydrogen reduction of magnetite

concentrate particles in the temperature range of 1423 K to 1673 K (1150 °C to 1400 °C),^[2,15] and that of hematite concentrate particles in the temperature range of 1423 K to 1623 K (1150 °C to 1350 °C).^[17] Most importantly, they have established that both magnetite and hematite concentrate can be reduced to more than 90 pct within several seconds, which presents sufficiently rapid kinetics for a flash reduction process.

As an integral part of the novel flash ironmaking process, the goal of this research was to perform a systematic measurement of the carbon monoxide reduction kinetics of hematite concentrate particles and derive the rate expression to eventually determine the kinetics rate expression for reduction by CO + H₂ mixtures. The carbon monoxide reduction kinetics of hematite concentrate particles in the temperature range 1473 K to 1623 K (1200 °C to 1350 °C) was determined. A rate equation that contains the effects of process variables in a flash ironmaking reactor, including process temperature and partial pressures of carbon monoxide and carbon dioxide, was developed.

II. EXPERIMENTAL WORK

A. Materials

Hematite concentrate used in this study was from the Yuanjiacun Range, Shanxi Province, China, which was the same raw material used in the study on hydrogen reduction kinetics.^[17] About 30 wt pct magnetite was originally contained in the ore and then removed by magnetic separation to separate hematite particles. The chemical composition of the magnetically concentrated hematite sample (about 88 wt pct hematite and 3.4 wt pct magnetite) is presented in Table I. The average particle size of the hematite concentrate was 21.3 μm. The size distribution is shown in Figure 1 as determined by a Hydro 2000MU particle size analyzer supplied by Malvern Instruments Ltd (Malvern, UK).

The carbon monoxide used in this study had a minimum purity of 99.95 pct. Nitrogen gas was added to vary the partial pressure of CO in the reduction process.

B. Experimental Apparatus

In order to accurately determine the chemical reaction rate of individual particles, the experimental reactor used a dilute particles-gas conveyed system in which fine particles flowed entrained in a reducing gas. The same high temperature drop-tube reactor (DTR) was previously used in the measurement of the H₂ reduction kinetics of magnetite concentrate by Choi and Sohn^[2] and Wang and Sohn^[15] as well as the H₂ reduction kinetics of hematite by Chen *et al.*^[17] The drop-tube reactor system consisted of a vertical tubular furnace housing an alumina tube (5.6 cm ID, 193 cm long), a pneumatic powder feeder, gas delivery lines, a powder cooling and collecting system, and an off-gas burning system, as shown in Figure 2.

The isothermal reaction zone of the alumina tube was maintained at a constant target temperature by rod-type

Table I. Chemical Composition of Hematite Concentrate Used in This Work

Component	Total Fe	FeO in Fe ₃ O ₄	SiO ₂	Al ₂ O ₃	K ₂ O	Na ₂ O	P	S
Wt pct	63.98	1.05	5.53	0.82	0.06	0.02	0.03	0.01

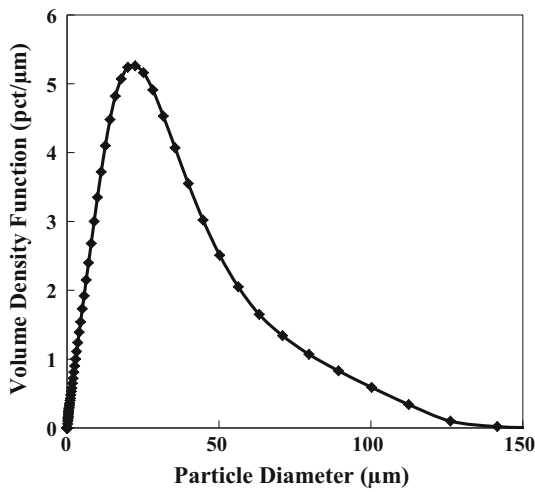


Fig. 1—Particle size distribution of hematite concentrate particles.

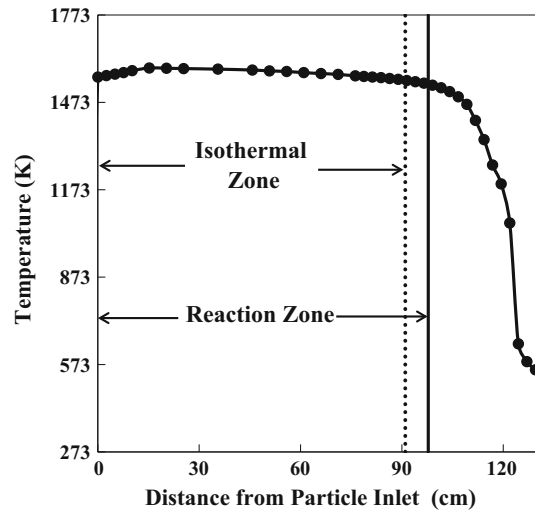


Fig. 3—Temperature profile of the drop-tube reactor with the isothermal zone at 1573 K (1300 °C) showing the corrected total reaction zone to account for gradual cooling after the isothermal zone.

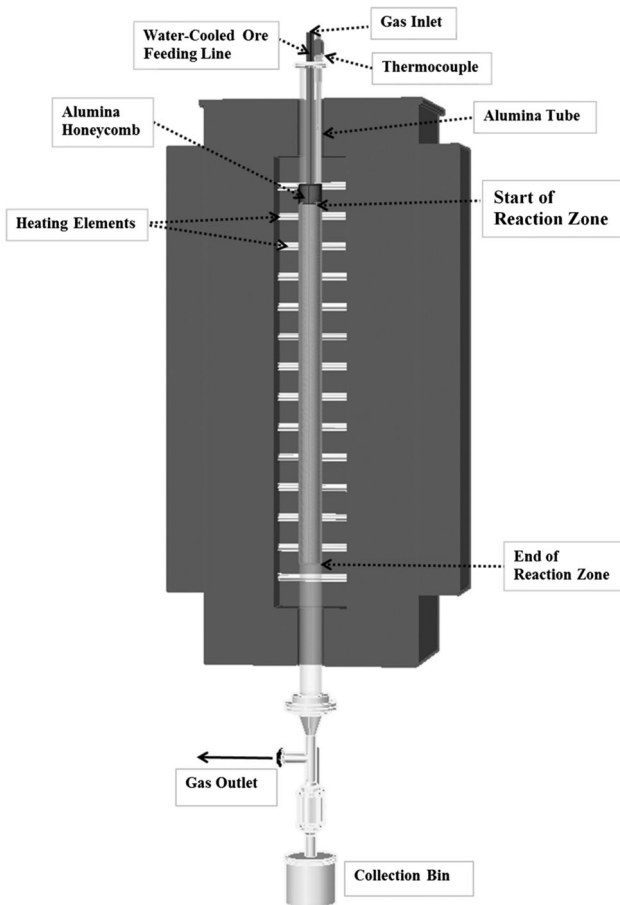


Fig. 2—Schematic diagram of the drop-tube reactor.

SiC heating elements. An alumina honeycomb had a hole in the middle for a water-cooled powder feeding line, and fixed at the beginning of the isothermal zone where the hematite particles are fed to the reaction tube. The isothermal zone (L_{iso}) where the temperature was maintained within ± 20 K started at the bottom of cylindrical honeycomb and extended 91 cm downward, as shown in Figure 2. The temperature decreased gradually after the end of the defined isothermal zone as the temperature profile measured at the center of reactor tube at all the experimental temperatures, and Figure 3 shows one example of the measured temperature profiles with the isothermal zone at 1573 K (1300 °C).

The isothermal zone was used in all the experimental design and analysis at first. Correction was then made to determine the initially obtained kinetic parameters taking into consideration the additional reduction that may occur in the 31 cm below the isothermal zone. A corrected rate expression, involving both the activation energy and pre-exponential factor, was then derived. The difference between the corrected and initial activation energy values was typically less than 1 pct. The procedure for this correction is discussed later in Section III-F.

The pneumatic powder feeding system consisted of a syringe pump, a vibrator, a carrier gas line, a powder container, and a powder delivery line. Dried concentrate particles were placed in a test tube (0.9 cm ID) and pushed up at a constant target advancing rate by the syringe pump to feed concentrate particles into the reactor tube with the help of vibration and the carrier gas (carbon monoxide/nitrogen or mixture) of a fixed

rate. The carrier gas entraining the powder passed through the powder delivery line (0.12 cm ID) and was fed into the reaction tube.

The reacted powder was collected in a powder collection bin at the bottom of the reactor. The excess carbon monoxide was combusted in the off-gas burning system.

C. Experimental Procedure

When the target temperature was reached, carbon monoxide and nitrogen were fed into the reactor at predetermined flow rates after the system was appropriately purged by nitrogen. After a thorough carbon monoxide leak test, the hematite particles were fed into the reactor tube. After a certain amount of the concentrate particles were supplied into the reactor, the syringe pump was stopped and the vibrator was kept running for 3 minutes longer to discharge the powder in the delivery lines. Then, carbon monoxide was closed and the flow rate of nitrogen increased to purge the whole system for 15 to 20 minutes. The valve of the powder collection bin was closed and the collector was disconnected from the reactor and quenched by water to room temperature to cool the reduced powder to avoid re-oxidation when the fine particles came into contact with air. The reduced sample was transferred to a vial sealed with a cap for further analysis by ICP, SEM, and XRD.

D. Sample Analysis

The total iron of the reduced sample was determined by ICP analysis to calculate the reduction degree from raw hematite to metallic iron. Spectro Genesis SOP spectrometer supplied by SPECTRO Analytical Instruments Inc. (Mahwah, NJ) was used for this analysis. To validate the analytical procedure, pure hematite with over 99 pct purity was analyzed after every five samples to detect any operator errors or bias in the analysis method. Random samples were duplicated and the reproducibility of the analysis method was within 1 pct.

Micrographs of reduced samples were taken by FEI Quanta 600 FEG SEM supplied by FEI (Hillsboro, Oregon). The SEM was equipped with an EDS tool, supplied by EDAX Inc. (Mahwah, NJ).

To identify the different phases in the partially reduced samples, the fine powder was analyzed using a Rigaku D/Max-2200V X-ray diffractometer supplied by Rigaku (The Woodlands, TX) and equipped with Ni-filtered Cu K α radiation ($\lambda = 1.5406 \text{ \AA}$). The X-ray intensity was measured over 2θ (θ : diffraction angle) from 10 to 90 deg with a scanning rate of 0.08 deg/s.

Carbon might be generated by the Boudouard reaction ($2\text{CO} \rightleftharpoons \text{CO}_2 + \text{C}$), thus carbon content in two representative samples, one of a high reduction degree [about 90 pct reduction under high CO partial pressure and 1623 K (1350 °C)] and the other had a low reduction degree, were analyzed by LECO CS244 supplied by LECO Corporation (St. Joseph, MI). The carbon content was 0.097 and 0.047 pct, respectively, and thus the carbon content was ignored in the analysis of reduced samples. This low level of carbon in the

product may be due to the fact that even the highly reduced sample still contained a significant amount of oxygen. Since the purpose of this work is to determine the kinetics during the main duration of the reduction reaction, it was not necessary to further examine the possibility of carbon absorption by a more highly reduced product.

E. Definition of Parameters

The degree of reduction was obtained from the difference of the mass of oxygen combined with iron in the concentrate particles before and after reduction. The amount of oxygen in the gangue materials that can be reduced by CO is negligible and the weight change due to the possible volatile species such as phosphorus and sulfur was also neglected based on the small contents in the chemical composition.

The expression for the degree of reduction is as follows:

$$\text{Degree of reduction} = \frac{m_o(0) - m_o(t)}{m_o(0)} \times 100 \text{ (pct)}, \quad [1]$$

$$m_o(0) = \frac{m_2}{x \text{ (pct)}} \times y \text{ (pct)}, \quad [2]$$

$$m_o(t) = m_1 - m_2 - \frac{m_2}{x \text{ (pct)}} \times z \text{ (pct)}, \quad [3]$$

where $m_o(0)$ is the mass of the removable oxygen in the sample before reduction corresponding to the amount of collected sample; $m_o(t)$ is the mass of the removable oxygen in reduced sample collected after reduction for time t ; m_1 is the mass of reduced sample used in the ICP analysis; m_2 is the mass of total iron in the reduced sample used in the ICP analysis; x (percent) is the mass percentage of total iron in the sample before reduction; y (percent) is the mass percentage of removable oxygen in the sample before reduction; z (percent) is the mass percentage of gangue in the sample before reduction;

$$x \text{ (pct)} + y \text{ (pct)} + z \text{ (pct)} = 100 \text{ (pct)}.$$

The residence time was calculated by considering the length of the reaction zone, the linear velocity of the gas and the terminal falling velocity of particles. Since the solid particles fall along the centerline of the reactor tube, the maximum velocity of the gas was used in the calculation, which is twice the average velocity (= volumetric flow rate divided by cross-sectional area). The terminal velocity of particles in the creeping flow regime was expressed by Stokes' law assuming that particles fall at a constant velocity in the isothermal zone. The following are the relevant equations for residence time calculation:

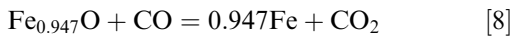
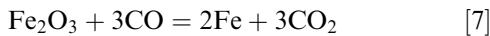
$$u_t = d_p^2 g (\rho_p - \rho_g) / 18\mu, \quad [4]$$

$$u_p = u_g + u_t, \quad [5]$$

$$\tau = L/u_p, \quad [6]$$

where d_p is the particle size, g the gravitational acceleration, ρ_p the particle density, ρ_g the gas density, μ the viscosity of the gas, u_p the particle velocity relative to tube wall, u_g the centerline gas velocity at furnace temperature, u_t the terminal velocity of a falling particle, τ is the residence time, and L is the length of the reaction zone.

To accurately determine the kinetics, it is best to carry out the experiment under a condition in which the gaseous reactant concentration remains essentially constant over the entire reactor length. This requires a sufficiently large excess of the gaseous reactant over the stoichiometric requirement. In some of the runs, the use of sufficiently large excess gas was not possible and a small concentration of carbon dioxide in the exit gas was expected. The final stage of hematite reduction, the reaction of $\text{Fe}_{0.947}\text{O}$ with carbon monoxide, is significantly limited by equilibrium (The values of K of the reaction between $\text{Fe}_{0.947}\text{O}$ and carbon monoxide at different temperatures are listed in Appendix). This equilibrium limitation was carefully considered in this study and it has led to the development of the pct excess carbon monoxide, defined as follows. The minimum amount of CO ($n_{\text{CO,min}}$) is the amount of carbon monoxide used to remove the oxygen from hematite, n_o , plus the amount required by the equilibrium of reaction^[8] below. The term pct excess CO was calculated from the total amount of carbon monoxide fed into the reaction ($n_{\text{CO,fed}}$) compared with the minimum amount of carbon monoxide, as shown in Eq. [10].



$$n_{\text{CO,min}} = n_o + \frac{n_{\text{CO}_2}}{K} \quad [9]$$

$$\text{pct excess CO} = \frac{n_{\text{CO,fed}} - n_{\text{CO,min}}}{n_{\text{CO,min}}} \times 100 \quad [10]$$

III. RESULTS AND DISCUSSION

A. Factors Affecting the Overall Rate

The hematite concentrate particles were entrained in the gas to transport down the reactor and reduced in-flight. If the reaction rate was controlled by external mass transfer and/or pore diffusion, it would take milliseconds to finish the reduction of a $\sim 20 \mu\text{m}$ particle.^[2] However, as observed in this study, several seconds were needed to fully reduce an individual particle. Thus, the overall reaction rate was controlled by the chemical reaction of individual particle. In order to examine the reduction behavior of the hematite

concentrate particles with carbon monoxide and obtain the rate expression, experiments to determine the effect of carbon monoxide partial pressure and reduction temperature on the reduction rate were conducted.

It is noted that the specific barometric pressure of Salt Lake City is 0.85 atm (1 atm = 101.32 kPa), which was used as the total pressure in all the experimental design and analysis in this work.

B. Reproducibility of Experimental Results

In experiments using a drop-tube reactor, only distinct points of different residence times at certain intervals can be obtained. The reproducibility of data needs to be checked under the same conditions. From the preliminary results using this experimental system, the reduction degree at every point was reproducible within ± 4 pct of the average reduction degree of three repeated experiments.

Figure 4 shows examples of the reduction degree of hematite vs residence time at different experimental conditions, and the lines correspond to calculated curves according to the complete rate equation developed subsequently, Eq. [23]. The entire experimental data of hematite reduction by CO obtained under various conditions are listed in Appendix.

C. Selection of Reduction Rate Model

A number of kinetic equations were tested on the obtained data to find the best-fitting equation: power law, contraction models, kinetics-order models, solid-state diffusion models, and the nucleation and growth model. From a mechanistic point of view, it is not uncommon in the gaseous reduction of fine metal oxide particles to follow the nucleation and growth process.^[15] Supported by, not only the goodness of the fit, but also by the SEM micrographs shown in Figure 5, the nucleation and growth model best represented the

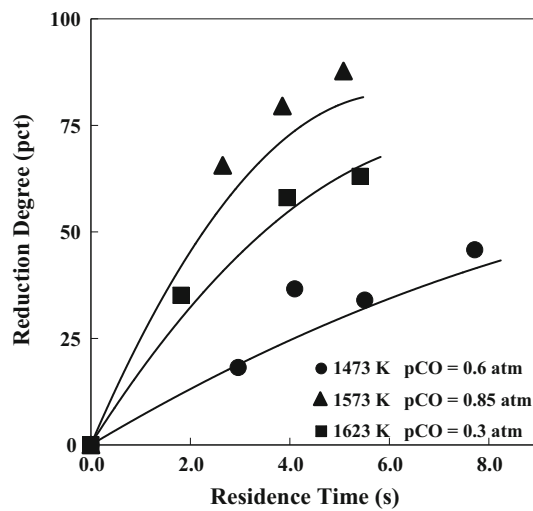


Fig. 4—Reduction degree of hematite vs residence time. The solid lines represent the calculated reduction degree using the developed rate expression, Eq. [23]. (pct excess CO > 500 in all experiments.)

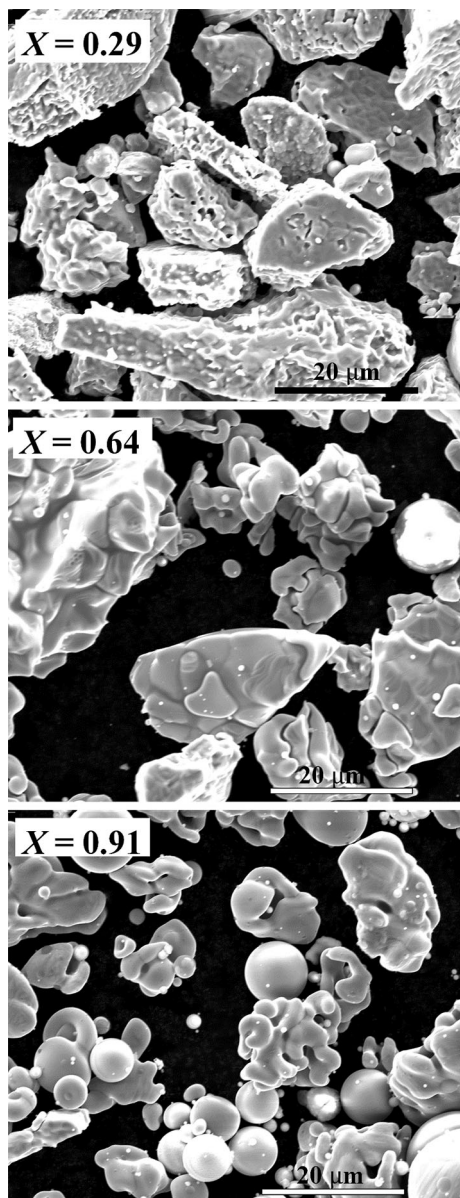


Fig. 5—SEM micrographs of samples with different reduction degrees in the temperature range 1473 K to 1623 K (1200 °C to 1350 °C) with p_{CO} from 0.3 to 0.85 atm. ($X = 0.29$: 1473 K (1200 °C), 4.3 s, $p_{\text{CO}} = 0.45$ atm; $X = 0.64$: 1573 K (1300 °C), 4.2 s, $p_{\text{CO}} = 0.60$ atm; $X = 0.91$: 1623 K (1350 °C), 5.7 s, $p_{\text{CO}} = 0.85$ atm).

kinetics of hematite concentrate reduction by carbon monoxide. In the previous work on the kinetics of hydrogen reduction of magnetite concentrate particles by Wang and Sohn^[15] and the kinetics of hydrogen reduction of hematite concentrate particles by Chen *et al.*,^[17] the nucleation and growth kinetics expression was also found to best represent the reduction kinetics. In the nucleation and growth kinetics, carbon monoxide is adsorbed on active sites on the surface and then reacts with oxygen and produces Fe nuclei that grow with time, as shown in Figure 5. For small particles, the period of the formation and growth of nuclei occupies essentially the entire conversion range. The

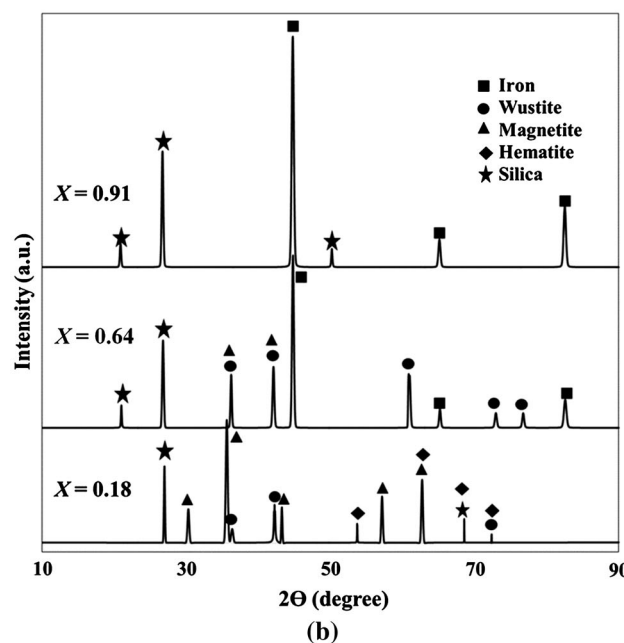
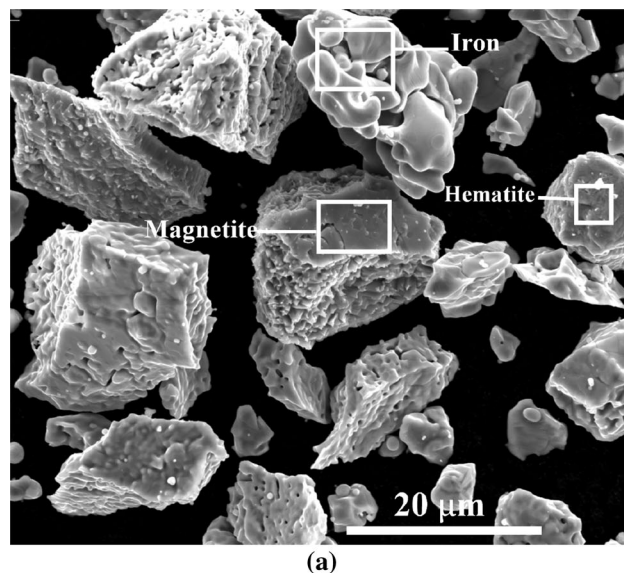


Fig. 6—Coexistence of various iron oxide phases along with iron as evidenced by: (a) SEM micrographs of reduced sample particles ($X = 0.18$) and (b) XRD (using Cu K α) of samples with different reduction degrees.

reduction of hematite to iron in the temperature range of this work proceeds through the formation of Fe_3O_4 and FeO with changes in reactivity. However, for small particles, it is extremely difficult to follow the irregular evolution of morphology involving Fe_3O_4 and FeO formation and the overlapping regions of different reduction extents. Furthermore, the reduction of Fe_2O_3 to FeO accounts for only the first 33 pct of conversion, whereas the main interest in this work and the new ironmaking technology is the attainment of high degrees of reduction. As mentioned above, a combination of hematite, magnetite, wustite, and iron is present at any given moment in the reduction of fine hematite particles, as evidenced by SEM-EDS and XRD, as

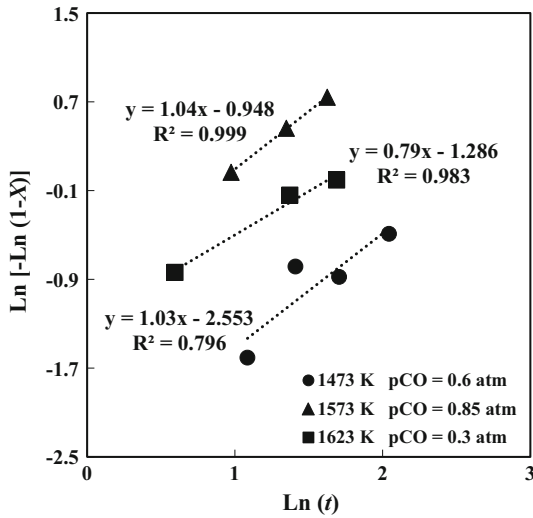


Fig. 7—Determination of Avrami parameter n under different experimental conditions. (t in seconds; pct excess CO > 500 in all experiments.).

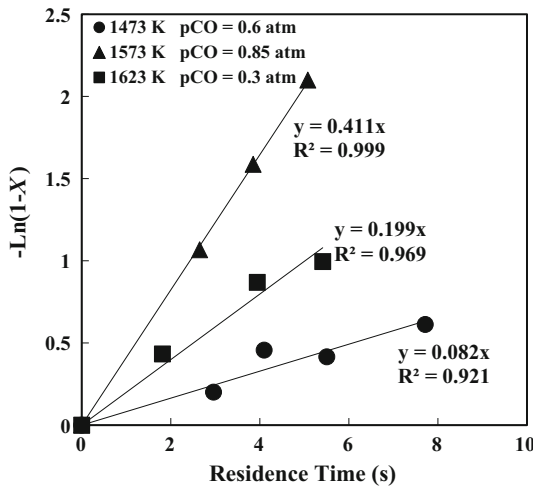


Fig. 8—Test of the Avrami parameter $n = 1$ under different experimental conditions.

shown in Figure 6. Thus, the following global nucleation and growth rate equation for the overall reduction process, as used in the hydrogen reduction kinetics of magnetite^[15] and hematite^[17], was also used in this work:

$$[-\ln(1-X)]^{1/n} = [k \times f_p(p\text{CO}, p\text{CO}_2)] \times t = k_{\text{app}} \times t, \quad [11]$$

where X is the fraction of oxygen removed from iron oxide (fractional degree of reduction); t is the residence time; n is the Avrami parameter; k is the rate constant; $f_p(p\text{CO}, p\text{CO}_2)$ is the concentration driving force; and k_{app} is the apparent rate constant.

When the temperature and carbon monoxide partial pressure are constant, we can calculate the Avrami parameter, n , from Eq. [11] as follows:

$$\ln[-\ln(1-X)] = n \times (\ln(t) + \ln(k_{\text{app}})) = n \times \ln(t) + C \quad [12]$$

In the original theoretical derivation, n was held to have an integer value between 1 and 4 which reflected the nature of the transformation in question;^[18–20] however, it has become customary to regard it as an adjustable parameter that may be non-integral.^[21] It was found that $n \approx 1$ was the average value from the experimental data; examples are shown in Figure 7. Thus, the value of $n = 1$ was used in all cases. There was a linear relationship with high R^2 values between $-\ln(1-X)$ and t under constant temperature and carbon monoxide partial pressures, as shown in Figure 8.

D. Determination of Reaction Order with Respect to CO Partial Pressure

From Eq. [11], the apparent rate constant can be expressed as follows:

$$k_{\text{app}} = k \times f_p(p\text{CO}, p\text{CO}_2) \quad [13]$$

Therefore, the relationship between k_{app} and $f_p(p\text{CO}, p\text{CO}_2)$ should be linear when the reduction temperature is fixed. The last step of iron oxide reduction ($\text{Fe}_{0.947}\text{O} + \text{CO} \rightleftharpoons 0.947 \text{Fe} + \text{CO}_2$) is equilibrium limited, which means that a negative term should be added to the carbon monoxide partial pressure to represent the lowering of the concentration driving force for the forward reaction due to the presence of CO_2 . Since the rate expression of a reaction must satisfy its equilibrium relationship, the exponent on the partial pressure of the product gas in the rate expression is fixed by a combination of the reaction order with respect to the carbon monoxide partial pressure and the equilibrium relationship.^[22] Thus, the dependence on gas partial pressures is expressed as follows:

$$f_p(p\text{CO}, p\text{CO}_2) = p\text{CO}^m - (p\text{CO}_2/K)^m, \quad [14]$$

where K is the equilibrium constant for the carbon monoxide reduction of $\text{Fe}_{0.947}\text{O}$, and m is the reaction order with respect to the partial pressure of carbon monoxide. The exponent of the two partial pressure terms must be equal to satisfy the equilibrium relationship $K = p\text{CO}_2/p\text{CO}$, as mentioned above. It is noted that the term with the negative sign in the rate expression for an equilibrium-limited gas–solid reaction does not represent the rate of the corresponding reverse reaction; rather, it represents the lowering of the concentration driving force for the net forward reaction due to the thermodynamic equilibrium limitation.^[22] The values of K at different temperatures are presented in Appendix.

The pct excess CO in all the experiments was higher than 500 based on complete reduction, and the CO_2 generated by the reduction was always less than 5 pct of the input carbon monoxide in the experimental runs.

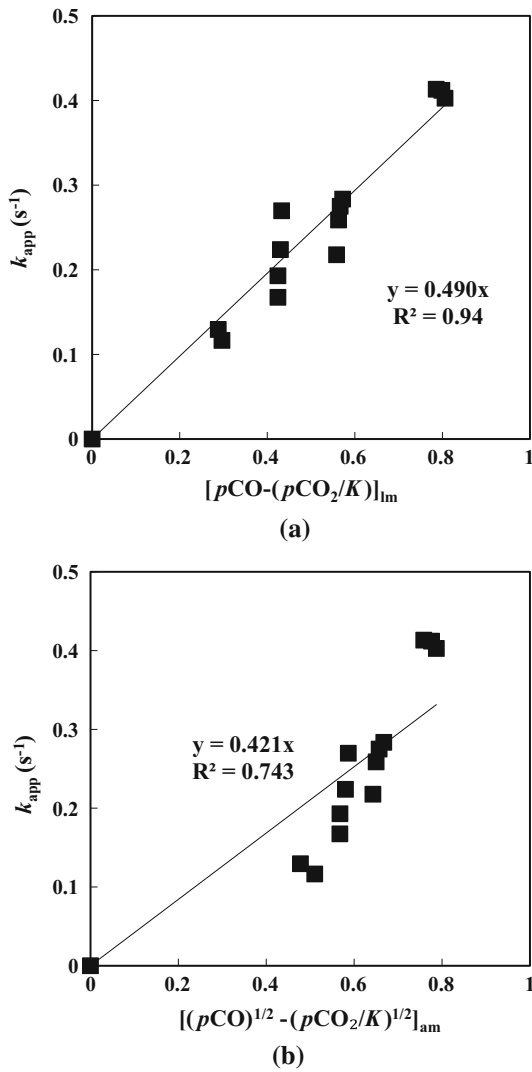


Fig. 9—Relationship between k_{app} and $f_p(pCO, pCO_2)$ at 1573 K (1300 °C) for different m values. (k_{app} in s^{-1} ; pCO, pCO_2 in atm.).

The effects of even such small changes were accounted for using the average concentration driving force between the inlet and exit values in the rate analysis, as shown below.

According to the amount of hematite powder fed ($n_{hematitefed}$) and its reduction degree (X) for a run, the amount of carbon dioxide generated (n_{CO_2}) and the partial pressure of carbon dioxide (p_{CO_2}) under the specific barometric pressure of Salt Lake City (0.85 atm) were calculated as follows:

$$p_{CO_2} = \frac{n_{CO_2}}{n_{CO_2} + n_{CO} + n_{N_2}} \times 0.85 \text{ atm} \quad [15]$$

$$n_{CO_2} = 3 \times n_{hematitefed} \times X \text{ mol} \quad [16]$$

$$n_{CO} = n_{CO, fed} - n_{CO_2} \text{ mol} \quad [17]$$

The partial pressure of CO in the inlet (p_{CO}) and the partial pressure of carbon dioxide generated in the

outlet (p_{CO_2}) are listed in Appendix. It was shown previously^[15] that a logarithmic or an arithmetic mean appropriately represents the average driving force, respectively, for first-order or half-order dependence with respect to the concentration driving force. Both first-order dependence and half-order dependence with respect to the partial pressure of CO was tested using the following relationships:

$$[f_p(pCO, pCO_2)]_{Avg} = [pCO - (pCO_2/K)]_{lm} \quad [18]$$

$$\text{or } [f_p(pCO, pCO_2)]_{Avg} = [pCO^{1/2} - (pCO_2/K)^{1/2}]_{am} \quad [19]$$

Taking the set of experiments at 1573 K (1300 °C) as an example, the k_{app} values obtained from Eq. [11] with $n = 1$ are plotted against $f_p(pCO, pCO_2)$ in Figure 9, which shows that $m = 1$ gives the best fit of the experimental data. Thus, hematite concentrate reduction is of first order with respect to carbon monoxide partial pressure in the ranges of conditions tested.

E. Determination of Activation Energy

After the functional dependence of rate on the partial pressures of carbon monoxide is determined, the reaction rate constant k can be obtained from Eq. [13].

$$k = \frac{k_{app}}{f_p(pCO, pCO_2)} = k_{app} / \left[pCO - \left(\frac{pCO_2}{K} \right) \right]_{lm} \quad [20]$$

$$k = k_0 \times e^{-\frac{E}{RT}} \quad [21]$$

$$\text{Ln } k = \text{Ln } k_0 - \frac{E}{RT} \quad [22]$$

Combining Eqs. [20] and [22], the activation energy is obtained from the slope of the plot of $\text{Ln } k$ vs $1/T$, which is shown in Figure 10. The value of activation energy was 233 kJ/mol and k_0 was 2.25×10^7 in the temperature range 1473 K to 1623 K (1200 °C to 1350 °C).

F. Correction for the Reaction Zone Length

The rate expression obtained above was based on the isothermal zone (L_{iso}). Considering that the isothermal zone does not end sharply and there is an additional temperature transition zone ($L_{trans} = 31$ cm), the effect of the latter on the calculated rate parameters was carefully analyzed.

The activation energy 233 kJ/mol was based on the assumption of a sharp temperature decrease after the isothermal zone and thus no further reaction. Considering the run for which the temperature of the isothermal zone was 1573 K (1300 °C) for example, the ratios of $e^{-\frac{E}{RT}}$ (T is the average temperature of the temperature measured in the additional zone every at intervals of 2.54 cm) to $e^{-\frac{E}{R \times 1573}}$ were obtained, then multiplied by a

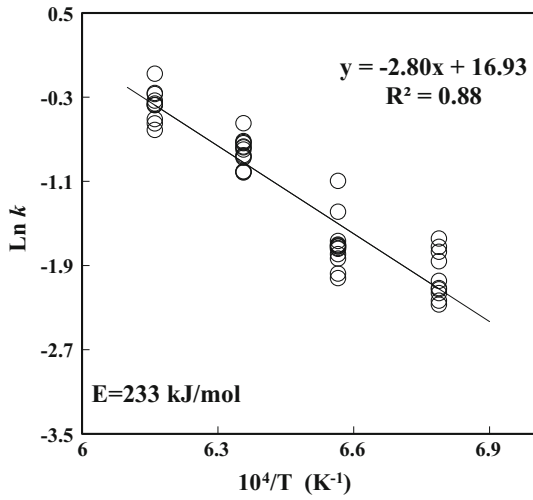


Fig. 10—Arrhenius plot between $\ln k$ and $10^4/T$. (k in atm^{-1}/s) Points at each temperature represent data under different CO partial pressures and reaction times. (Activation Energy of 233 kJ/mol is before reaction zone correction, and the final activation energy is 231 kJ/mol after correcting the reaction zone.)

temperature factor (=target temperature 1573 K (1300 °C)/measured temperature T to account for the effect of temperature on the gas velocity and thus the residence time at each interval), and the point at which the accumulated effect of the additional zone was half the total was chosen as the end of the actual reaction zone. The length representing the total ‘reaction zone’ was 98.1 cm instead of 91 cm for the isothermal zone at 1573 K (1300 °C). The calculation details are shown in Table II. The lengths of the total reaction zones thus calculated for runs at different temperatures are list in Table III, which were used to re-analyze all the experimental data to obtain the following corrected rate expression:

$$-\ln(1 - X) = 1.91 \times 10^7 \times e^{\frac{-231000}{RT}} \times \left(p_{\text{CO}} - \frac{p_{\text{CO}_2}}{K} \right)_{lm} \times t, \quad [23]$$

where R is 8.314 J/mol K, T is in K, p is in atm, and t is in seconds.

The instantaneous rate of reaction, which is valid under varying temperature and gas composition, is given by:

$$\frac{dX}{dt} = 1.91 \times 10^7 \times e^{\frac{-231000}{RT}} \times \left(p_{\text{CO}} - \frac{p_{\text{CO}_2}}{K} \right) \times (1 - X) \quad [24]$$

The value of corrected activation energy as obtained using the corrected total reaction zone was 231 kJ/mol, compared with 233 kJ/mol obtained using the ‘isothermal zone’ of 91 cm. The difference in the calculated values of activation energy is less than 1 pct. If this difference was much greater, an iterative process would be necessary to obtain a more correct value of activation energy. Although the correction on the pre-exponential

Table II. Correction for Rate Determination at 1573 K (1300 °C)

Distance from Particle Inlet (cm)	Distance from the End of the ‘Isothermal Zone’ (cm)	T [K (°C)]	Average Distance from Particle Inlet (cm)	Average Distance from the End of the ‘Isothermal Zone’ (cm)	Average T (K)	$e^{\frac{E}{RT}}$	$e^{\frac{E}{RT}}$	$\left(\frac{e^{\frac{E}{RT}}}{e^{\frac{E}{RT_{1573}}}} \right)^{\frac{1573}{T}}$	Accumulated Additional Effect	Distance from Particle Inlet at Half Accum (cm)
91.4	0	1548 (1275)								
94.0	2.5	1544 (1271)	92.7	3.8	1546	1.34×10^{-8}	1.34×10^{-8}	0.7454	0.75	
96.5	5.1	1539 (1266)	95.3	6.4	1541.5	1.27×10^{-8}	1.27×10^{-8}	0.7090	1.45	
99.1	7.6	1532 (1259)	97.8	8.9	1535.5	1.18×10^{-8}	1.18×10^{-8}	0.6630	2.12	
101.6	10.2	1523 (1250)	100.3	11.4	1527.5	1.08×10^{-8}	1.08×10^{-8}	0.6057	2.72	
104.1	12.7	1510 (1237)	102.9	14.0	1516.5	9.42×10^{-9}	9.42×10^{-9}	0.5341	3.26	
106.7	15.2	1492 (1219)	105.4	16.5	1501	7.79×10^{-9}	7.79×10^{-9}	0.4459	3.70	
109.2	17.8	1466 (1193)	108.0	19.1	1479	5.90×10^{-9}	5.90×10^{-9}	0.3428	4.05	
111.8	20.3	1411 (1138)	110.5	21.6	1438.5	3.46×10^{-9}	3.46×10^{-9}	0.2067	4.25	
114.3	22.9	1345 (1072)	113.0	24.1	1378	1.47×10^{-9}	1.47×10^{-9}	0.0917	4.34	
116.8	25.4	1258 (985)	115.6	26.7	1301.5	4.45×10^{-10}	4.45×10^{-10}	0.0294	4.37	
119.4	27.9	1193 (920)	118.1	29.2	1225.5	1.17×10^{-10}	1.17×10^{-10}	0.0082	4.38	
121.9	30.5	1059 (786)	120.7	31.8	1126	1.55×10^{-11}	1.55×10^{-11}	0.0012	4.38	98.1

Table III. Corrected Lengths of Reaction Zone at Different Temperatures

Temperature [K (°C)]	1473 (1200)	1523 (1250)	1573 (1300)	1623 (1350)
Length of reaction zone (cm)	97.2	97.6	98.1	97.9

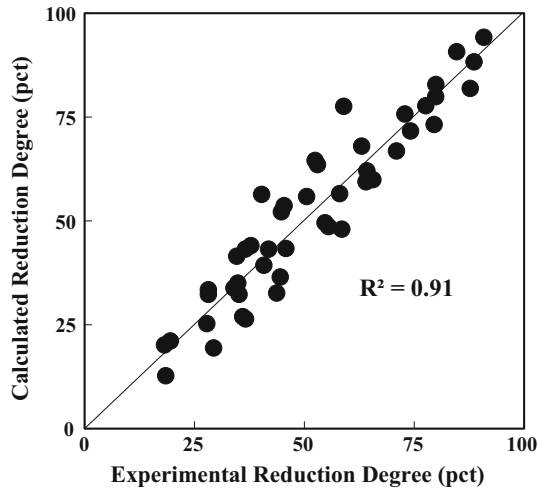


Fig. 11—Comparison between the calculated reduction degree (using Eq. [23]) and the experimental results for all the runs made in this work.

factor is larger, no iteration is necessary because this value is simply inversely proportional to the residence time based on the corrected total length of the ‘reaction zone’. Equation [24] is the final rate expression for the reduction degrees of hematite in the temperature range 1473 K to 1623 K (1200 °C to 1350 °C).

G. Comparison of Experimental and Calculated Results

A comparison between the experimental values of the reduction degree and those calculated by the rate expression developed above using Eq. [23] is shown in Figure 11. The calculated results represent the experimental results quite well. In addition, as shown in Figure 4, the agreement between the calculated reduction degrees vs time using the developed rate equation and the experimental results is satisfactory.

H. Comparison with Related Previous Work

The hydrogen reduction kinetics of hematite concentrate particles was studied by Feng *et al.*^[17] In that work, $n = 1$ was also the Avrami parameter that best fitted the data. Further, the hematite reduction rate had a first-order dependence on the partial pressure of hydrogen. The hydrogen reduction rate expression of hematite concentrate particles is as follows:

$$-\ln(1 - X) = 4.41 \times 10^7 \times e^{\frac{-214000}{RT}} \times \left(p_{\text{H}_2} - \frac{p_{\text{H}_2\text{O}}}{K} \right)_{lm} \times t, \quad [25]$$

where R is 8.314 J/mol K, T is in K, p is in atm, and t is in seconds.

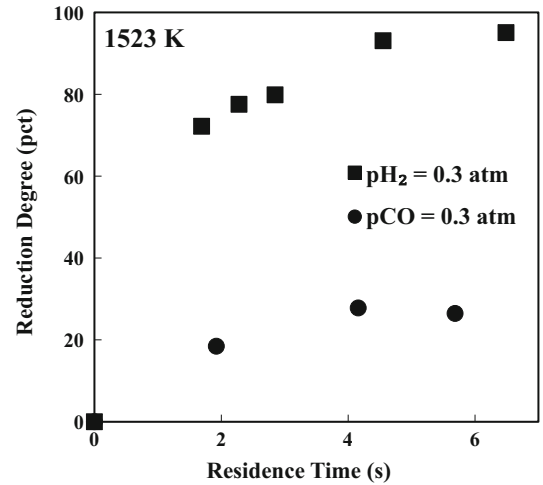


Fig. 12—Experimental reduction degrees of hematite vs residence time with H₂ and CO under different experimental conditions.

Compared with the activation energy of the hydrogen reduction of hematite concentrate of 214 kJ/mol in the temperature range 1423 K to 1623 K (1150 °C to 1350 °C), it can be seen that the carbon monoxide reduction of hematite concentrate has slightly higher activation energy, which is 231 kJ/mol in the temperature range 1473 K to 1623 K (1200 °C to 1350 °C). It can be seen that the activation energy of the hydrogen reduction of hematite particles is close to that of carbon monoxide. This is attributed to the fact that the reduction reaction in case H₂ or CO comes down the removal of oxygen from Fe_{0.947}O. The examples of reduction degree of hematite vs residence time with H₂ and CO are shown in Figure 12.

The ratio between the rate constants for reduction by hydrogen and by carbon monoxide (k_{H_2} and k_{CO}) is shown in Eq. [26] and Table IV.

$$\text{Ratio} = \frac{k_{\text{H}_2}}{k_{\text{CO}}} = \frac{4.41 \times 10^7 \times e^{\frac{-214,000}{RT}}}{1.91 \times 10^7 \times e^{\frac{-231,000}{RT}}} = 2.31 \times e^{\frac{17,000}{RT}} \quad [26]$$

k_{H_2} is approximately 9 times k_{CO} in the temperature range of 1423 K to 1623 K (1150 °C to 1350 °C).

The values of activation energy obtained by others who studied the reduction of iron oxide by CO were smaller than that obtained in this work, 231 kJ/mol.^[8–14] Bohn and Cleeton^[12] found the value of activation energy to be 90 ± 29 kJ/mol for the step of Fe₃O₄ reduction to Fe_{0.947}O in the overall reduction of hematite in carbon monoxide and carbon dioxide mixtures in a fluidized bed. They found that the reduction reaction was first order with respect to the concentration of CO which is consistent with our

Table IV. Relationship Between the Rate Constants of H₂ and CO at Different Temperatures

Temperature [K (°C)]	1423 (1150)	1473 (1200)	1523 (1250)	1573 (1300)	1623 (1350)
Ratio = $\frac{k_{H_2}}{k_{CO}}$	9.72	9.26	8.84	8.48	8.14

findings in this work. However, it is difficult to compare our results to their other kinetic parameters due to lower temperatures and larger size of particles (300 to 425 μm) used in their work. Further, the reaction of particles in a fluidized bed is prone to the effect of mass transfer^[23], which would lower the observed activation energy.

IV. CONCLUDING REMARKS

The carbon monoxide reduction kinetics of hematite concentrate of an average particle size 21.3 μm in the temperature range 1473 K to 1623 K (1200 °C to 1350 °C) was investigated. The reduction of hematite particles by carbon monoxide is slower than that by hydrogen. Besides, the reduction of Fe_{0.947}O by CO is greatly limited by equilibrium. However, hematite concentrate particles still can be reduced to >90 pct by carbon monoxide in several seconds of residence time typically available in a flash reactor. Thus, it is significant to determine carbon monoxide kinetics of hematite reduction separately from hydrogen to help understand and analyze the complex kinetics of hematite reduction by the H₂ + CO mixtures.

The nucleation and growth rate equation with an Avrami parameter *n* = 1 well described the carbon monoxide kinetics of hematite reduction at different temperatures and partial pressures of carbon monoxide. The reduction rate has a 1st-order dependence on the partial pressure of carbon monoxide. The activation energy of carbon monoxide reduction of hematite concentrate was 231 kJ/mol in contrast to 214 kJ/mol for the hydrogen reduction as previously determined. Overall, the reduction rate of hematite concentrate by carbon monoxide is slower than by hydrogen. An overall rate equation was obtained, which satisfactorily represented the carbon monoxide reduction kinetics of hematite concentrate particles.

ACKNOWLEDGMENTS

The authors thank Andrew Laroche, Omar Kergaye, and Mohamed El-Zohiery for help with the chemical analysis using ICP and the experimental runs. In addition, the authors would like thank the staff of Micron Microscopy Core at the University of Utah, especially Dr. Brian Van Devener, for the valuable help with SEM imaging. Feng Chen acknowledges the financial support from China Scholarship Council for her work at the University of Utah. This work was supported in part by the U.S. Department of Energy under Award Number DE-EE0005751 together with the generous cost share contributions by AISI (American Iron and Steel Institute) and the University of Utah.

DISCLAIMER

This report was prepared as an account of work sponsored by an agency of the United States Government. Neither the United States Government nor any agency thereof, nor any of their employees, makes any warranty, express or implied, or assumes any legal liability or responsibility for the accuracy, completeness, or usefulness of any information, apparatus, product, or process disclosed, or represents that its use would not infringe privately owned rights. Reference herein to any specific commercial product, process, or service by trade name, trademark, manufacturer, or otherwise does not necessarily constitute or imply its endorsement, recommendation, or favoring by the United States Government or any agency thereof. The views and opinions of authors expressed herein do not necessarily state or reflect those of the United States Government or any agency thereof.

APPENDIX: COMPLETE EXPERIMENTAL DATA (EXCESS CARBON MONOXIDE > 500 PCT)

Temp. [K (°C)]	<i>K</i> of Fe _{0.947} O Reduction*	<i>p</i> CO (atm)	<i>p</i> CO ₂ (atm)	Residence Time (s)	Solid Feeding Rate (mg/min)	CO Flow Rate (L/min)**	Fractional Reduction Degree		
1473 (1200)	0.3109	0.45	0.007	9.1	49	0.7	0.45		
			0.006	6.3	84	1.1	0.36		
			0.004	4.3	115	1.7	0.29		
			0.012	8.6	85	1.0	0.46		
			0.007	6.1	102	1.5	0.34		
			0.007	4.6	143	2.1	0.37		
		0.60	0.85	0.85	0.003	3.3	177	3.0	0.18
					0.015	8.7	97	1.4	0.51
					0.011	6.0	143	2.2	0.42
					0.011	4.5	221	3.0	0.35

Temp. [K (°C)]	K of Fe _{0.947} O Reduction*	pCO (atm)	pCO ₂ (atm)	Residence Time (s)	Solid Feeding Rate (mg/min)	CO Flow Rate (L/min)**	Fractional Reduction Degree	
1523 (1250)	0.2941	0.30	0.002	6.5	42	0.7	0.26	
			0.003	4.8	75	1.0	0.28	
			0.002	2.2	143	2.3	0.18	
		0.45	0.006	9.1	49	0.7	0.40	
			0.007	6.3	100	1.1	0.37	
			0.005	4.3	126	1.7	0.28	
			0.004	2.5	212	3.0	0.26	
			0.60	0.011	8.6	70	1.0	0.52
				0.011	6.1	122	1.5	0.45
		0.007		4.8	128	2.0	0.38	
		0.85	0.003	3.3	121	3.0	0.28	
			0.013	8.7	74	1.4	0.59	
			0.017	6.0	173	2.2	0.53	
			0.016	4.5	255	3.0	0.45	
			0.012	3.1	376	4.5	0.35	
1573 (1300)	0.2792		0.30	0.005	6.3	56	0.7	0.39
				0.005	4.6	84	1.0	0.41
				0.002	2.1	120	2.3	0.20
			0.45	0.011	8.8	47	0.7	0.73
		0.011		6.0	85	1.1	0.64	
		0.009		4.1	118	1.7	0.55	
		0.007		2.4	228	3.0	0.44	
		0.60		0.018	8.4	75	1.0	0.80
				0.016	5.9	109	1.5	0.74
			0.014	4.2	166	2.2	0.64	
		0.85	0.012	3.2	221	3.0	0.55	
			0.026	8.0	109	1.4	0.78	
			0.027	5.8	163	2.2	0.88	
			0.022	4.4	197	3.0	0.80	
			0.019	3.0	308	4.5	0.66	
1623 (1350)	0.2657		0.30	0.006	6.2	49	0.7	0.63
		0.006		4.5	69	1.0	0.58	
		0.004		2.1	164	2.3	0.35	
		0.45	0.012	8.8	44	0.7	0.85	
			0.014	6.0	85	1.1	0.80	
			0.011	4.0	117	1.7	0.71	
			0.010	2.4	223	3.0	0.59	
			0.85	0.023	7.9	85	1.4	0.91
				0.030	5.7	172	2.2	0.91
		0.032		4.3	255	3.0	0.89	
		0.026	3.0	356	4.5	0.78		

* HSC 5.11^[24] was used to calculate equilibrium constants.

** Flow rates were calculated at 298 K (25 °C) and 0.85 atm (1 atm = 101.32 kPa).

REFERENCES

1. H.Y. Sohn: *Steel Times Int.*, 2007, vol. 31 (4), pp. 68–72.
2. M.E. Choi and H.Y. Sohn: *Ironmaking Steelmaking*, 2010, vol. 37 (2), pp. 81–88.
3. H.K. Pinegar, M.S. Moats, and H.Y. Sohn: *Steel Res. Int.*, 2011, vol. 82 (8), pp. 951–63.
4. M.Y. Mohassab Ahmed: Ph.D. Dissertation, The University of Utah, Salt Lake City, UT, 2013.
5. M.Y. Mohassab-Ahmed and H.Y. Sohn: *JOM*, 2013, vol. 65 (11), pp. 1559–65.
6. M.Y. Mohassab-Ahmed and H.Y. Sohn: *Steel Res. Int.*, 2014, vol. 85 (5), pp. 875–84.
7. M.Y. Mohassab-Ahmed and H.Y. Sohn: *Ironmak. Steelmak.*, 2014, vol. 41 (9), pp. 665–75.
8. H.S. Ray and N. Kundu: *Thermochim. Acta*, 1986, vol. 101, pp. 107–18.
9. S.K. Dutta and A. Ghosh: *ISIJ Int.*, 1993, vol. 33 (11), pp. 1168–73.
10. K. Piotrowski, K. Mondal, T. Wiltowski, P. Dydo, and G. Rizeg: *Chem. Eng. J.*, 2007, vol. 131 (1–3), pp. 73–82.
11. A. Bonalde, A. Henriquez, and M. Manrique: *ISIJ Int.*, 2005, vol. 45 (9), pp. 1255–60.
12. C.D. Bohn, J.P. Cleeton, C.M. Müller, S.A. Scott and J.S. Dennis: *Proceedings of the 20th International Conference on Fluidized Bed Combustion*, 2009, pp. 555–61.
13. K. Mondal, H. Lorethova, E. Hippo, T. Wiltowski, and S.B. Lalvani: *Fuel Process. Technol.*, 2004, vol. 86 (1), pp. 33–47.
14. R. Corbari and R.J. Fruehan: *Metall. Mater. Trans. B*, 2009, vol. 41B, pp. 318–29.
15. H. Wang and H.Y. Sohn: *Metall. Mater. Trans. B*, 2013, vol. 44B, pp. 133–45.
16. M.E. Choi, H.Y. Sohn, and G. Han: in *Sohn International Symposium Advanced Processing of Metals and Materials Vol.*

- 2—*Thermo and Physicochemical Principles: Iron and Steel Making*, F. Kongoli and R.G. Reddy, eds., TMS (The Minerals, Metals & Materials Society), Warrendale, PA, pp. 105–10, 2006.
17. F. Chen, Y. Mohassab, M. Olivas-Martinez, T. Jiang and H.Y. Sohn: *Metall. Mater. Trans. B*, in press.
 18. M. Avrami: *J. Chem. Phys.*, 1939, vol. 7 (12), pp. 1103–12.
 19. M. Avrami: *J. Chem. Phys.*, 1940, vol. 8 (2), pp. 212–24.
 20. M. Avrami: *J. Chem. Phys.*, 1941, vol. 9 (2), pp. 177–84.
 21. Compendium of Chemical Terminology: *IUPAC Recommendations*, A.D. McNaught and A. Wilkinson Blackwell Science Malden, Massachusetts, 1997, p. 35.
 22. H.Y. Sohn: *Metall. Mater. Trans. B*, 2014, vol. 45B, pp. 1600–1602.
 23. D. Kunii and O. Levenspiel: *Fluidization Engineering*, Wiley, New York, 1969, pp. 195–210.
 24. A. Roine: *HSC Chemistry*, Ver. 5.11, Outokumpo, Pori, Finland, 2002.